# Investigation of the Minimum Conditions for Reliable Estimation of Clinically Relevant HRV Measures

## *Introducing a Novel Approach to the Validation of HRV Measurement Systems*

Esben Ahrens[1], Helge B. D. Sorensen[1], Henning Langberg[2], Karsten Hoppe[3] and Dorthe Bodholt Saadi[3]

[1]*Department of Electrical Engineering, Technical University of Denmark, Ørsteds Plads Building 348, 2800 Kgs. Lyngby, Denmark*

[2]*Department of Public Health, Copenhagen University, Henrik Pontoppidansvej 4, 1014 Copenhagen K, Denmark*

[3]*DELTA Danish Electronics, Lights & Acoustics, Venlighedsvej 4, 2970 Hørshom, Denmark*

Keywords: Heart Rate Variability, Jitter, Ectopic Beat.

Abstract: The R-peak localization error (jitter) of a heart rate variability (HRV) system has a great impact on the values of the HRV measures. Only a few studies have analyzed this subject and purely done so from the aspect of choice of sampling frequency. In this study we provide an overview of the various factors that comprise the jitter of a system. We propose a method inspired by the field of signal averaged electrocardiography (SAECG) that allows for a quantification of the jitter of any HRV system that records and stores the raw ECG signal. Furthermore, with this method the differences between the HRV measures of the system and HRV measures corresponding to the physiological truth can be quantified. The method is used to obtain the physiologically true R-peak locations of subjects from Physionet's 'Normal Sinus Rhythm Database'. The effects of jitter are then analyzed via mathematical modelling for short-term and long-term HRV for various HRV measures. The effects of abnormal beats and missed and false detections are analyzed as well.

## 1 INTRODUCTION

Evaluation of heart rate variability (HRV) has been acknowledged to provide a reliable reflection of the autonomic modulation of the normal heart rhythm. Different HRV measures have thus been suggested to contain clinically relevant information about diseases related to autonomic dysfunction, e.g. assessment of diabetic neuropathy (AHA and ESC, 1996). One of the major HRV research areas is related to risk stratification in populations with myocardial infarction, congestive heart failure, or left ventricular dysfunction. A brief review of the most relevant studies related to this risk stratification is provided in (Huikuri and Stein, 2013). They generally find that based on the available data, abnormal HRV measures are a general risk factor for cardiac death in patients after myocardial infarction (Huikuri and Stein, 2013). However, they also note that most observational studies achieve low sensitivity and low negative predictivity for adverse outcomes using HRV measures (Huikuri and Stein, 2013). This suggests that more research and methodological development is needed in this area. As a part of a continued research effort, we therefore consider it highly relevant to take a closer look at the prerequisites for obtaining reliable HRV measures. This reliability is primarily limited by the ability to obtain uninterrupted and accurate series of normal RR intervals (Citi et al., 2012). Furthermore, the emergence of HRV analysis in various health management applications makes it highly relevant to obtain greater knowledge about the minimum conditions needed to obtain reliable estimates of HRV measures.

**Causal Analysis of NN Series Errors.** The quality of the obtained NN (normal-to-normal) series might be reduced by several different sources of error. Figure 1 gives an overview of these sources. One of the main contributors to errors in the NN series is the interruptions caused by QRS detection errors or abnormal beats.

The other main contributor to errors in the NN series is jitter (localization error) in the automatic detection of the exact R-peak location. This jitter might be caused by imprecise digitization of the true phy-



Ahrens, E., Sorensen, H., Langberg, H., Hoppe, K. and Saadi, D..
Investigation of the Minimum Conditions for Reliable Estimation of Clinically Relevant HRV Measures - Introducing a Novel Approach to the Validation of HRV Measurement Systems.
In *Proceedings of the 3rd International Congress on Cardiovascular Technologies (CARDIOTECHNIX 2015)*, pages 30-38
ISBN: 978-989-758-160-1

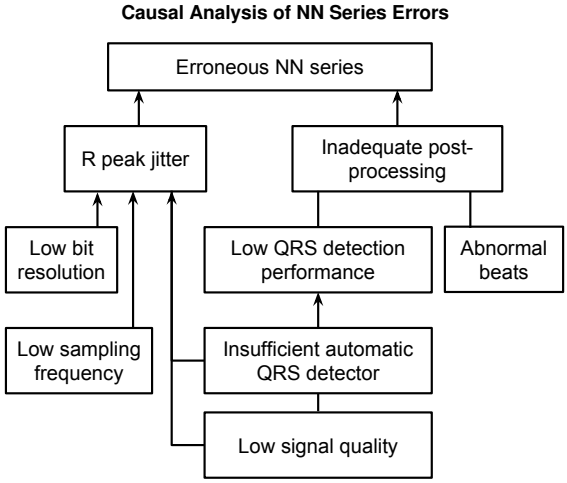


Figure 1: Overview of the most important potential causes of errors in the NN series. The presence of each of these errors might influence the reliability of the estimated HRV measures. Low QRS detection performance refers to the effect of false and/or missing R-peak detections.

siological R-peak and/or by imprecise fiducial point localization provided by the automatic QRS detector. The accuracy of the digitization depends on both the sampling frequency and the resolution of the applied electrocardiography (ECG) recorder. These effects are illustrated in Figure 2. It is observed that the exact location of the digitized R-peak is highly dependent on a combination of the sampling frequency and the resolution. This poses a clear risk of inducing jitter. But jitter also depends on the fiducial points set by the QRS detector. Jitter might also arise from artifacts in the ECGs. Only a few studies have attempted to estimate the influence of the introduced jitter (Tapanainen et al., 1999) and most of them are primarily focused on the influence of the sampling frequency (García-González et al., 2004; Ziemssen et al., 2008). Only very limited knowledge is available about the influence of the overall amount of jitter. There are thus several unanswered questions related to the necessary prerequisites for reliable estimation of clinically relevant HRV measures. The focus of this study is therefore to provide new knowledge about the required minimum conditions that permit reliable estimation of clinically relevant HRV measures and a method capable of assessing whether or not these conditions are met.

## 2 METHODS

In (AHA and ESC, 1996) it is suggested that HRV measurement systems should be tested using simulated RR series with known HRV properties. One of the downsides to this approach is the lack of physio-

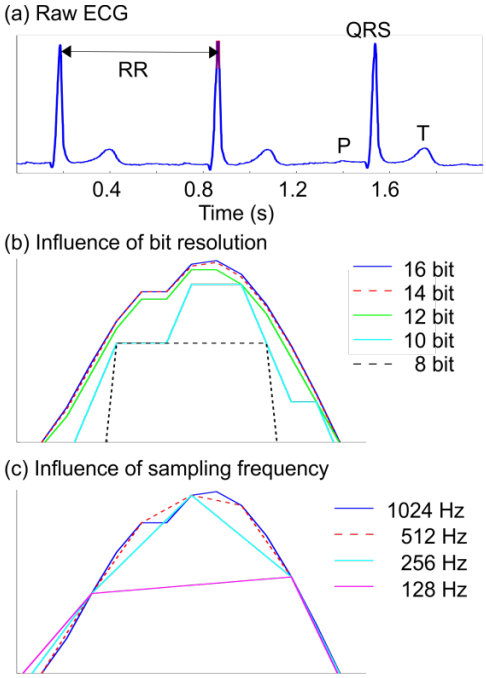


Figure 2: Illustration of the potential issues with imprecise digitization of the true physiological R-peak position. (a) Raw ECG snippet with indication of the most important ECG fiducial points. The red mark on top of the second QRS complex indicates the area that is zoomed in on in (a) and (b). (a) and (b) illustrate the influence of different bit resolutions and different sampling frequencies, respectively. The recorded reference curve is the blue line (16 bit, 1024 Hz), and the other curves are simulations based on the blue line.

logical relevance in the simulated signals. This fact is demonstrated by (Smith et al., 2002). Their method automatically classifies an RR series as synthetic or physiological. It yielded a 100% accuracy when evaluated on a Physionet/Computing in Cardiology 2002 challenge dataset. Hence, validation of HRV system using synthetic RR series as a basis may not be relevant for physiological ECG signals. Therefore, we suggest an alternative approach avoiding synthetic data.

A method that is very popular in the literature regarding signal averaged ECG (Fonseca et al., 2014; Shaw and Savard, 1995) is used to obtain the physiologically true R-peak locations. In contrast to simulated RR series, this data will contain relevant physiological content. The method obtains the true R-peak locations from raw ECG and QRS fiducial points. The true R-peak locations can then be used to calculate the jitter of an HRV measurement system. The jitter is defined as the standard deviation of the differences between the true R-peak locations and the fiducial points given by the system. Furthermore, physiologically true HRV measures based on the true RR series can be used to calculate the error of the HRV measurement system.

The method is then applied to Physionet's 'Normal Sinus Rhythm Database' in order to obtain physiologically true RR series with the locations of abnormal beats annotated as well. From the true RR series analyses of the effects of jitter and appropriate handling of abnormal beats, as well as missed and false detections are performed.

## 2.1 Obtaining the True RR Series

This section describes the cross correlation-based template matching algorithm. Baseline drift of the raw ECG is removed by filtration with a Kaiser window finite impulse response high-pass filter with a cut off frequency at 0.67 Hz. An example of input to the template matching algorithm is shown in Figure 3(a). The initial fiducial points could be manual annotations or output from an automatic QRS detector. Selected illustrative stages of the algorithm are shown in Figure 3 and the algorithm is defined by the following steps.

1. Interpolate the ECG signal such that the sampling frequency is increased to $f_{s_{\text{up}}} = 8192$ Hz. See Figure 3(b).
2. Extract a window of length equal to the median heartbeat interval around each of the current fiducial points. See Figures 3(b) and 3(c).
3. Calculate the template defined as the mean of the extracted windows. See Figure 3(d).
4. Calculate the cross correlation between the ECG signal around the estimated R-peak locations and the template. The sample index of the maximum cross correlation values is applied to improve the estimation of the R-peak location. These R-peak location estimations serve as the new fiducial points. See Figure 3(e).
5. Repeat steps 2.–4. once more.

Repeating steps 2.–4. a third time did not change the outcome. The output is compared with the input in Figure 3(f). The location of the physiologically true R-peak is defined by the template maximum (green cross). Note that it is located between the original samples of the raw ECG.

**Interpolation.** The database is sampled at 128 Hz. Since the frequency content of the QRS complex falls below half of this sampling frequency, the Shannon-Nyquist sampling theorem tells us that the signal can be reconstructed for all time by bandlimited interpolation (Dodson, 1992; Proakis and Monolakis, 1996; Bashir et al., 2010). Therefore, the interpolation in step 1 is performed by bandlimited interpolation.

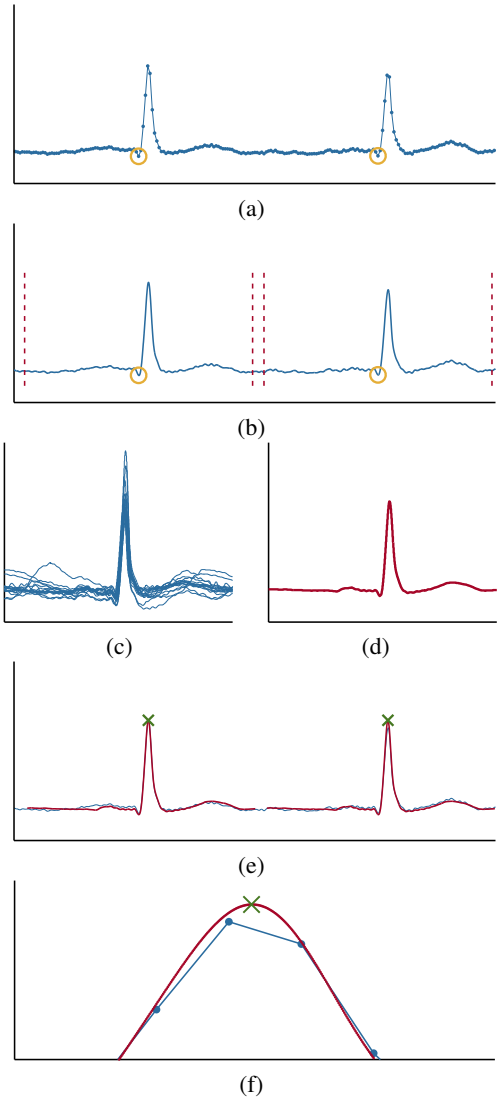


Figure 3: Illustration of the template matching algorithm described in section 2.1. (a) shows the ECG after removal of baseline drift, and manually annotated QRS complex fiducial points. (b) shows the interpolated ECG with fiducial points. The windows extracted in step 2 are marked by red, dotted lines. (c) shows examples of windows of interpolated ECG extracted in step 2. (d) shows the mean of the extracted windows of the interpolated ECG. This is the initial ECG template. (e) shows the interpolated ECG, and the initial template at the locations of maximal cross correlation. The template maximum is marked. It represents the result after steps 2.–4. have been executed once. These results serve as input when repeating the steps 2.–4. (f) shows a comparison between the original data and the algorithm output. The template (red line) and the physiologically true R-peak position (green cross) is shown along with the original raw ECG (blue line). Each blue dot indicates the location of one of the original samples. Note that the true R-peak position defined by the algorithm is in between two of the original samples.

In (Fonseca et al., 2014) a post-processing algorithm for precise R-peak location without the use of interpolation is introduced. However, the template matching algorithm is also used in (Fonseca et al., 2014) as a "golden standard" and is thus preferred here.

## 2.2 HRV Measures

For this study HRV measures from both the time (SDNN, RMSSD, pNN50, SDI), frequency (LF/HF, VHF), geometric ($\pi$SD1SD2), and non-linear domain was chosen (ApEn, SampEn).

SDNN is the standard deviation of all normal-to-normal (NN) intervals. RMSSD is the root-mean-square of the differences between successive NN-intervals. pNN50 is the percentage of differences between successive NN-intervals that are larger than 50 ms. SDI is the mean of all SDNN calculated over 5 minute intervals across a long-term recording.

The following ranges are used for frequency domain analysis: Very low frequency (VLF) [0.003, 0.04], low frequency (LF) [0.04, 0.15], high frequency (HF) [0.15, 0.4], and very high frequency (VHF) [0.4, 0.5]. The frequency spectrum was obtained both by Lomb-Scargle (L-S) periodogram and Fourier transformation of the RR time series equidistantly sampled at 4 Hz by using cubic spline interpolation. The L-S periodogram has the benefit of not requiring an equidistantly sampled time series.

SD1 is the standard deviation of the distances of the points of the Poincaré plot projected onto the identity line (x=y) and is related to short-term HRV. SD2 is the standard deviation of the distances of the points of the Poincaré plot projected onto the line perpendicular to the identity line and is related to long-term HRV. $\pi$SD1SD2 is calculated as $\pi \cdot \mathrm{SD1} \cdot \mathrm{SD2}$ and measures the overall variability.

Approximate entropy (AnEn) quantifies the unpredictability of fluctuations in the RR series. Sample entropy (SampEn) is a refined version of approximate entropy (Richman and Moorman, 2000).

## 2.3 Jitter Simulation

To investigate the effects of jitter a simulation of jitter is executed. Physionet's 'Normal Sinus Rhythm database' (Goldberger et al., 2000) contains both the raw ECG signals and annotations of 21 subjects and serves as a basis for the simulation. The physiologically true R-peak locations are found via the automatic template matching algorithm applied to the QRS complex fiducial points marked in the annotation files. In some areas the Normal Sinus Rhythm Database has marked normal QRS-complexes as being 'QRS-like artifacts'. We corrected this manually in order to obtain RR series free of any technical errors and excluded some subjects because of wrongful annotations. The RR series were detrended by a method based on smoothness priors (Tarvainen et al., 2002).

Table 1: Optimal jitter values assuming smallest possible jitter within the given sampling frequency. Average of jitter values for the Pan-Tompkins algorithm for the first two hours of the selected subjects of the dataset. Some subjects of the dataset were excluded because of wrongful annotations in the corresponding annotation files.

| $f_s$ (Hz) | Optimal jitter (ms) | Pan-Tompkins jitter (ms) |
|---|---|---|
| 128 | 2.3 | 8.8 |
| 256 | 1.1 | 4.3 |
| 512 | 0.6 | 1.8 |
| 1024 | 0.3 | 0.7 |

It is assumed that the jitter is normally distributed. Thus, the jitter simulation is carried out by adding random numbers drawn from the normal distribution to the true R-peak locations using a random number generator in MATLAB® (Mersenne Twister). This means that the simulation will only be exact for HRV systems that show the same pattern in their differences from the true R-peak locations. The simulation is run with increasing jitter values and it is repeated ten times for each jitter value. For each run relative accuracy error (RAE) is calculated as

$$\mathrm{RAE} = \frac{|s - s_{\mathrm{true}}|}{s_{\mathrm{true}}} \cdot 100\%, \tag{1}$$

for each estimated HRV measure $s$ and ground true HRV measure $s_{\mathrm{true}}$. Finally the average RAE is calculated over the ten runs at each level of jitter.

**Minimum Jitter.** Let the jitter be defined as the standard deviation of the localization errors of the R-peak fiducial points. Assume that the true RR series is known. Let the ECG signal be sampled at finite sampling frequency $f_s$. Theoretical jitter values can then be calculated assuming that the R wave fiducial point localization was ideal within the respective sampling frequency. The error will then be uniformly distributed on $[0, 1/f_s[$ and the standard deviation equals (Kellogg, 1996)

$$\frac{1/f_s}{\sqrt{12}}. \tag{2}$$

The jitter values given in Table 1 are found via this formula. It must be emphasized that these values represent best case scenarios.

**Jitter of the Pan-Tompkins Algorithm.** An implementation of the Pan-Tompkins QRS detector (Pan and

Tompkins, 1985) was tested on the data and compared to the ground truth. The different sampling frequencies were obtained by interpolation. This revealed the jitter values shown in the last column of Table 1. The values are much higher than the minimum values. The differences between the physiological truth and the fiducial points given by Pan-Tompkins were normally distributed, hence the output of the later described jitter simulation is accurate for this algorithm.

**Handling Abnormal Heartbeats.** Ectopic beats do not originate from the sinoatrial node, and the effect of these should therefore be minimized or eliminated when calculating the HRV measures. The abnormal beats (e.g. ectopic beats) are marked in the annotations file. From this information an investigation on the effect of adjusting the respective RR time events (outliers) versus leaving the RR series unaltered for both short-term and long-term HRV was performed.

For time series analysis the outliers were deleted prior to calculation of the HRV measures. For frequency spectrum analysis, the outliers were replaced by cubic spline interpolation when calculating the equidistantly sampled RR series. For geometric and nonlinear measures the outliers were replaced using cubic spline interpolation.

**Missed & False Detections.** Missed and false QRS detections are simulated by extracting a random 5 minute RR series free of abnormal beats from each subject and randomly removing or adding an extra beat. The added beat is restricted to not being closer than 250 ms to any neighboring beat. This simulates a refractory period typically implemented in an automatic QRS detector. Automatic outlier detection and replacement methods for manipulation of the RR series can be found in e.g. (Kemper et al., 2007).

# 3 RESULTS & DISCUSSION

## 3.1 Jitter

Subsets of the results of the short-term and long-term HRV jitter simulations are shown in Figure 5 and 6, respectively. Figure 4 explains how Figure 5 and 6 should be read. The short-term HRV error is calculated as the mean error of the HRV measures of 5-minute segments selected randomly as the beginning of each of the first ten hours of the recordings which all start before noon, yielding a total of ten segments for each subject. For each chosen subject and HRV measure the average relative accuracy error (RAE) is shown as

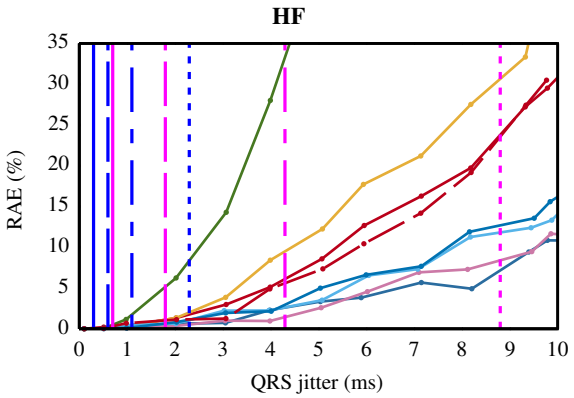


Figure 4: This figure and text explains how Figures 5 and 6 should be read. The blue vertical lines represent minimum (which also means optimal) jitter values at sampling frequencies 1024, 512, 256, and 128 Hz from left to right. The magenta lines represent jitter values of the tested Pan-Tompkins algorithm at the same sampling frequencies and illustrates that the jitter at various sampling frequencies depends on the QRS detector. Note that each sampling frequency is illustrated by a distinct line style. It is apparent that the relative accuracy error (RAE) does not only depend on sampling frequency, but on the system as a whole. On Figures 5 and 6 the lines marking the Pan-Tompkins algorithm performance are left out. The acceptable level of RAE will be application dependent. This graph shows the jitter simulation output of one HRV measure (HF) for a subset of subjects from the database. Only eight subjects are included in this illustrative graph for the sake of clarity. A large inter-subject variability is seen. Furthermore, it is seen that the relative accuracy error (RAE) increases as the jitter increases.

a function of increasing jitter. The minimum jitter at sampling frequencies 1024, 512, 256 and 128 Hz is shown as the blue lines from left to right. Figures 5(a) and 6(a) show the measured jitter of the tested implementation of the Pan-Tompkins algorithm as the magenta lines. This illustrates that the jitter does not only depend on the choice of sampling frequency but of many other factors, one being the performance of the QRS detector.

In general, the results of the two simulations are quite close to each other. However, the curves of the long-term simulation are smoother. This is probably because of the simulated noise is randomly chosen from the normal distribution. Longer segments will create empirical distributions quite close to the normal distribution, while shorter segments might not. This illustrates how the instability of a system can have a greater impact on HRV analysis on shorter segments. There are large interpersonal variations in the relative accuracy errors (RAE) for all simulations.

A HRV measure like pNN50 can quite quickly have a large RAE since the respective NN50 count can e.g. be equal to 1 and adding e.g. 1 more as a

result of noise can then double the RAE. This shows that conclusions based on pNN50 should be made with care, especially for short-term HRV, see Figures 5(c) and 6(c).

The jitter induced changes in the LF/HF measure are dominated by HF. LF, VLF, and ULF are quite stable in regards to jitter as could be expected. Since HF is overestimated at higher levels of jitter, LF/HF is underestimated as a result, see Figures 5(b), 6(b), and 6(d). VHF is affected to a greater degree by jitter than HF, which shows that jitter induced by e.g. lower sampling frequency adds high frequency noise — the higher the frequencies in question the greater the error, see Figure 5(d). Frequency domain measures based on L-S periodogram and Fourier transformation were strikingly similar as illustrated by Figures 6(d) and 6(b). This was surprising since the L-S method does not require the step of obtaining an equidistantly sampled RR series. The error in the measure $\pi$SD1SD2 is dominated by SD1 measuring short-term variability and will be overestimated as a result of jitter, see Figures 5(g) and 6(g). It is thought by some to give a better estimate of the overall variability as compared to SDNN, but it is not as stable in regards to jitter, see Figures 5(a) and 6(a). SDI is as stable as SDNN, which could be expected, see Figure 6(f). RMSSD is very similar to $\pi$SD1SD2 in the way that it is calculated and thus not surprisingly also in jitter sensitivity, see Figure 6(e).

**Sampling Frequency.** It is interesting to note that inducing jitter, e.g. by lowering the sampling frequency, will have the effect of overestimating most of the HRV measures. This means that a perfect QRS detector will potentially be able to detect the high frequency fluctuations of the HRV measures with greater accuracy at higher sampling frequencies, and inducing jitter by lowering the sampling frequency and/or decreasing the localization accuracy of the QRS detector can result in overestimation of the HRV measures designed to measure high frequency fluctuations.

As discussed, the jitter might originate from several different factors (e.g. low bit resolution, low sampling frequency, artefacts, and low QRS localization accuracy). These factors are mutually influencing each other, and it is thus difficult to provide a definitive conclusion on the required sampling frequency independently of all other factors in the HRV measurement system. We therefore recommend that the cumulative effect from all factors are investigated when choosing the sampling frequency.

**Abnormal Heartbeats.** Table 2 on page 9 shows the average plus/minus the standard deviation of the relative accuracy error for all subjects. It is clear that the effect of not correcting the abnormal beats in the short-term HRV can be quite severe. The long-term analysis is more robust for this type of error with a maximum value of 2%. This suggests that when performing short-term HRV analysis on healthy subjects biological errors need to be addressed. However, for long-term analysis on this dataset the effects of abnormal beats are deemed to be insignificant.

**Missed & False Detections.** The effects of a missed detection are higher than that of a false detection, see Table 2. It is interesting to see that a missed detection also has a profound effect on LF, while a false detection has much less. Overall the errors are very high except for the HRV measure meanNN. It is clear that such an error will have a much more serious negative effect on the HRV measures than the choice of lower sampling frequency of e.g. 128 Hz. This can also be observed on SDNN which proved to be very stable when higher levels of jitter were applied.

**Comparison with Existing Literature.** In (Ziemssen et al., 2008) the EUROBAVAR data set, sampled at 500 Hz, is downsampled to 200 Hz and 100 Hz. Only ultra high frequency (defined by frequencies $> 40$ Hz) was significantly different when comparing the values across the different sampling frequencies. This is comparable to our results, where VHF shows larger errors than LF/HF at the same jitter levels, see Figure 5. In (AHA and ESC, 1996) it is recommended to use RMSSD instead of pNN50, since it has better statistical properties. In (Hejjel and Roth, 2004) the authors find that pNN50 is very unreliable even at jitter levels of 1 ms. This is also supported by our results.

# 4 CONCLUSION

We recommend that each HRV measurement system should be validated by

1. showing low jitter levels, and/or
2. the HRV measures that it produces should be compared with and be close to the ones obtained by the template matching method described in this study.

This method will allow HRV systems to be tested without the need for synthetic signals or comparison with a different system recording simultaneously. It only requires access to the recorded ECG signal.

In this study it was found that handling abnormal beats was important for short-term HRV analysis, but

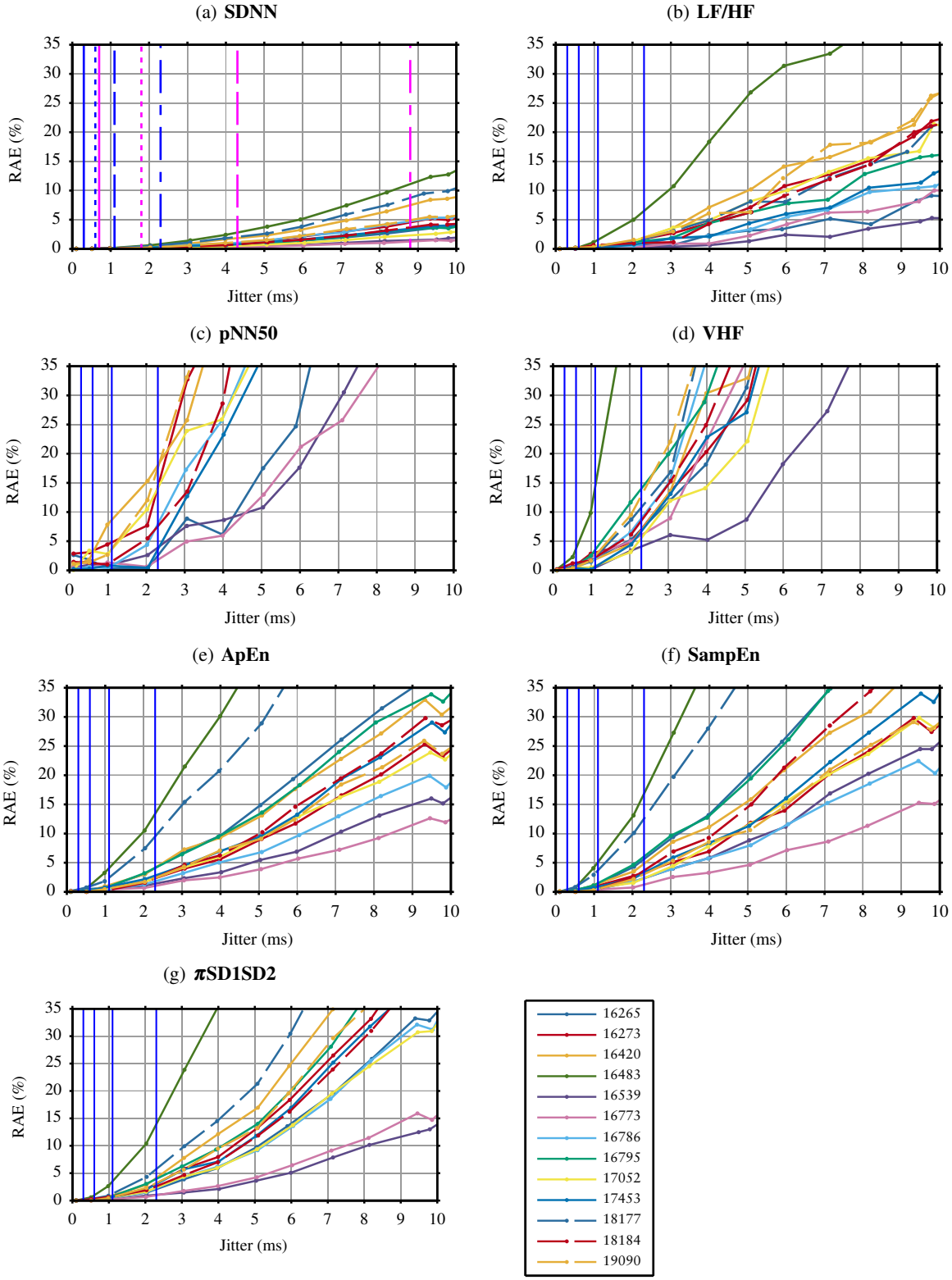


Figure 5: Jitter simulations based on short-term HRV measures. The average relative accuracy error (RAE) is shown as a function of jitter for different subjects. The blue lines correspond to minimal possible jitter at sampling frequencies 1024, 512, 256, and 128 Hz from left to right. (a) also shows the jitter of the Pan-Tompkins algorithm — note the matching line styles between the sampling frequencies. The subject identification numbers are shown in the legend.

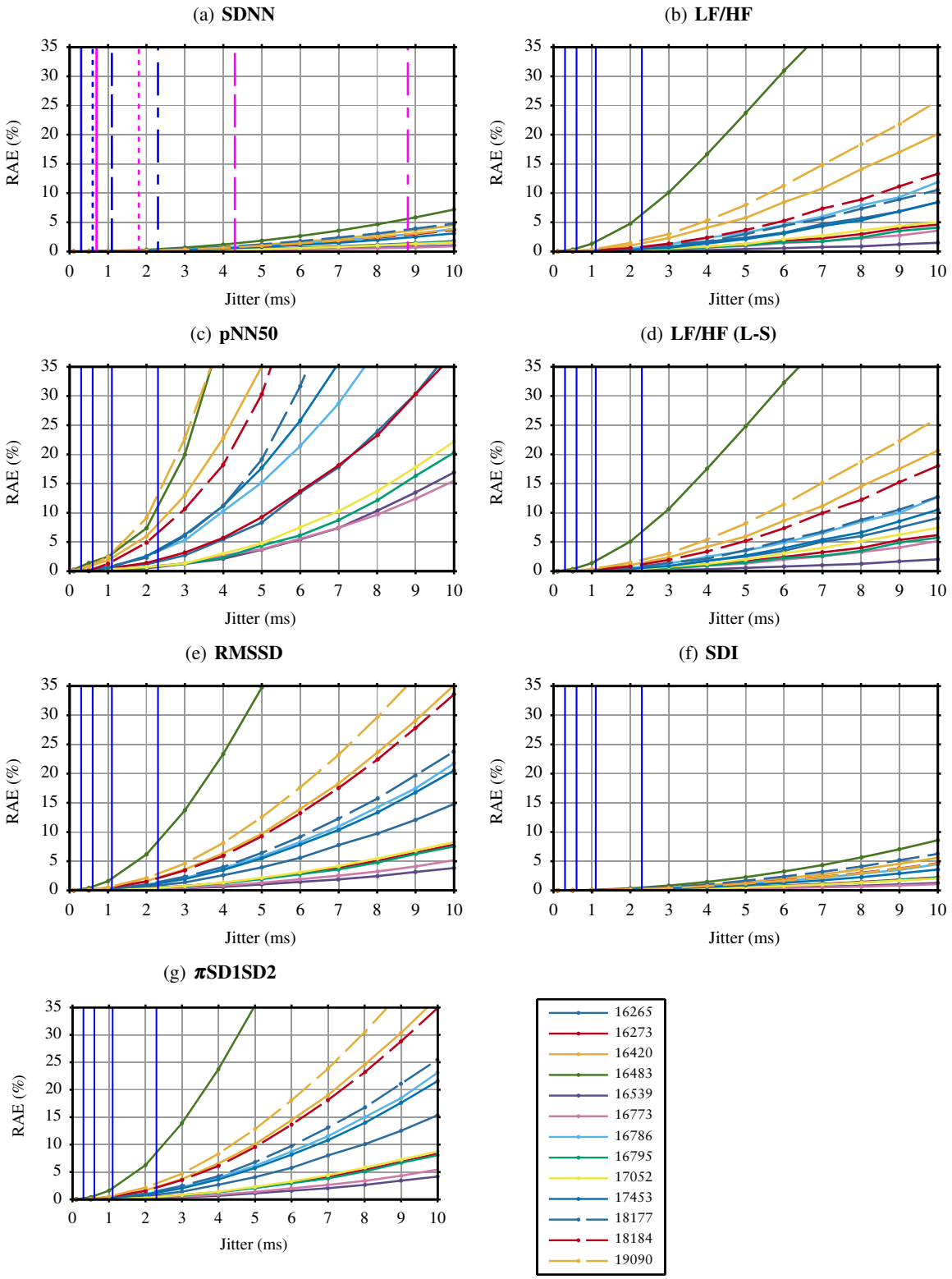


Figure 6: Jitter simulations based on long-term HRV measures. The average relative accuracy error (RAE) is shown as a function of jitter for different subjects. The blue lines correspond to minimal possible jitter at sampling frequencies 1024, 512, 256, and 128 Hz from left to right. (a) also shows the jitter of the Pan-Tompkins algorithm — note the matching line styles between the sampling frequencies. The subject identification numbers are shown in the legend.

Table 2: Average plus/minus standard deviation of relative approximation error in percent for both abnormal beats, false and missed detections.

| | meanNN | SDNN | RMSSD | pNN50 | HF | LF | $\pi$SD1SD2 |
|---|---|---|---|---|---|---|---|
| **Abnormal beat** | | | | | | | |
| Long-term | $0.0 \pm 0.0$ | $0.1 \pm 0.1$ | $0.6 \pm 0.6$ | $0.2 \pm 0.4$ | $0.4 \pm 0.5$ | $0.1 \pm 0.1$ | $0.5 \pm 0.6$ |
| Short-term | $0.0 \pm 0.0$ | $1.6 \pm 1.7$ | $11.6 \pm 11.1$ | $7.6 \pm 14.6$ | $14.1 \pm 15.2$ | $4.1 \pm 8.0$ | $12.4 \pm 11.3$ |
| **False detection** | | | | | | | |
| Short-term | $0.2 \pm 0.0$ | $7.9 \pm 7.0$ | $53.7 \pm 51.2$ | $15.5 \pm 13.8$ | $85.1 \pm 124.1$ | $6.0 \pm 4.6$ | $64.0 \pm 62.5$ |
| **Missed detection** | | | | | | | |
| Short-term | $0.2 \pm 0.0$ | $15.8 \pm 17.6$ | $128.7 \pm 102.7$ | $11.8 \pm 10.9$ | $657.6 \pm 1119.7$ | $83.8 \pm 91.9$ | $158.9 \pm 155.0$ |

not for long-term HRV. It was found that missed and false detection had a severe effect on short-term HRV.

We cannot define a limit for acceptable jitter levels because it will depend on the analysis carried out in each the specific study.

This investigating was carried out using ECG from healthy subjects. The results are therefore limited to studies using healthy subjects. Analysis of subjects with lower HRV measures might result in larger relative errors at the same levels of jitter.

# REFERENCES


Bashir, M., Lee, D., Akasha, M., Yi, G., Cha, E., Bae, J., Cho, M., and Ryu, K. (2010). Highlighting the current issues with pride suggestions for improving the performance of real time cardiac health monitoring. Information Technology in Bio-and Medical Informatics, ITBAM 2010, pages 226–233.

ESC and NASPE (1996). Guidelines Heart rate variability. *European Heart Journal*, pages 354–381.

Citi, L., Brown, E. N., and Barbieri, R. (2012). A real-time automated point-process method for the detection and correction of erroneous and ectopic heartbeats. *IEEE Transactions on Biomedical Engineering*, 59(10):2828–2837.

Dodson, M. (1992). Shannon's Sampling Theorem. Current Science, 63(5):253 – 260.

Fonseca, P., Aarts, R. M., Foussier, J., and Long, X. (2014). A novel low-complexity post-processing algorithm for precise QRS localization. *SpringerPlus*, 3(1):376.

García-González, M. a., Fernández-Chimeno, M., and Ramos-Castro, J. (2004). Bias and uncertainty in heart rate variability spectral indices due to the finite ECG sampling frequency. *Physiological measurement*, 25(2):489–504.

Goldberger, A., Amaral, L., Glass, L., Hausdorff, J., Ivanov, P., Mark, R., Mietus, J., Moody, G., Peng, C.-K., and Stanley, H. (2000). PhysioBank, PhysioToolkit, and PhysioNet: Components of a New Research Resource for Complex Physiologic Signals. *Circulation*, 101(23):e215–e220.

Hejjel, L. and Roth, E. (2004). What is the adequate sampling interval of the ECG signal for heart rate variability analysis in the time domain? Physiological measurement, 25(6):1405–1411.

Huikuri, H. V. and Stein, P. K. (2013). Heart rate variability in risk stratification of cardiac patients. *Progress in Cardiovascular Diseases*, 56(2):153–159.

Kellogg, B. (1996). CRC Standard Mathematical Tables and Formulae (Daniel Zwillinger, ed.).

Kemper, K. J., Hamilton, C., and Atkinson, M. (2007). Heart rate variability: Impact of differences in outlier identification and management strategies on common measures in three clinical populations. *Pediatric Research*, 62(3):337–342.

Pan, J. and Tompkins, W. J. (1985). A real-time QRS detection algorithm. IEEE transactions on bio-medical engineering, 32(3):230–236.

Proakis, J. G. and Monolakis, D. G. (1996). Digital Signal Processing: principles, algorithms and applications.

Richman, J. S. and Moorman, J. R. (2000). Physiological time-series analysis using approximate entropy and sample entropy. *American journal of physiology. Heart and circulatory physiology*, 278(6):H2039–H2049.

Shaw, G. R. and Savard, P. (1995). On the detection of QRS variations in the ECG. *IEEE Transactions on Biomedical Engineering*, 42(7):736–741.

Smith, F. E., Bowers, E. J., Langley, P., Allen, J., and Murray, A. (2002). Heart rate variability characteristics required for simulation of interval sequences. In *Computers in Cardiology*, volume 29, pages 237–240.

Tapanainen, J. M., Seppänen, T., Laukkanen, R., Loimaala, A., and Huikuri, H. V. (1999). Significance of the accuracy of RR interval detection for the analysis of new dynamic measures of heart rate variability. *Annals of Noninvasive Electrocardiology*, 4(1):10–18.

Tarvainen, M. P., Ranta-Aho, P. O., and Karjalainen, P. A. (2002). An advanced detrending method with application to HRV analysis. *IEEE transactions on biomedical engineering*, 49(2):172–5.

Ziemssen, T., Gasch, J., and Ruediger, H. (2008). Influence of ECG sampling frequency on spectral analysis of RR intervals and baroreflex sensitivity using the EUROBAVAR data set. *Journal of Clinical Monitoring and Computing*, 22(2):159–168.